

FULL PAPER

Plasma-treated polyethylene as electrochemical mediator for enzymatic glucose sensors: Toward bifunctional glucose and dopamine sensors

Jorge J. Buendía^{1,2,3} | Georgina Fabregat^{1,2} | Alejandra Castedo^{2,3} |
Jordi Llorca^{2,3} | Carlos Alemán^{1,2} 

¹ Departament d'Enginyeria Química, EEBE, Universitat Politècnica de Catalunya, C/Eduard Maristany, 10-14, Ed. I2, Barcelona 08019, Spain

² Barcelona Research Center in Multiscale Science and Engineering, Universitat Politècnica de Catalunya, C/Eduard Maristany, 10-14, Barcelona 08019, Spain

³ Institut de Tècniques Energètiques, EEBE, Universitat Politècnica de Catalunya, C/Eduard Maristany, 10-14, Ed. C3, Barcelona 08019, Spain

Correspondence

Georgina Fabregat, Jordi Llorca, and Carlos Alemán, Barcelona Research Center in Multiscale Science and Engineering, Universitat Politècnica de Catalunya, C/Eduard Maristany, 10-14, Barcelona 08019, Spain.

Email: georgina.fabregat@upc.edu (GF); jordi.llerca@ucp.edu (JL); carlos.aleman@upc.edu (CA)

Funding information

Secretaría de Estado de Investigación, Desarrollo e Innovación, Grant number: MAT2015-69367-R

The application of inert and insulating low density polyethylene (LDPE) in electrochemical detection is null. However, in a recent study it was found that reactive species formed onto the surface of plasma-treated LDPE and other polymers promote the electrocatalytic oxidation of dopamine. In this work, we examine the role of plasma-treated LDPE as mediator in enzymatic glucose biosensors based on Glucose oxidase and glass carbon substrate. Results indicate that plasma-induced changes facilitate the electrocommunication between the enzyme and the substrate. The chronoamperometric response of these sensors prove their bifunctionality since the oxidation of glucose to gluconolactone, which is catalyzed by the GOx, coexists with the oxidation of dopamine that is electrocatalyzed by the plasma activated LDPE surface.



KEYWORDS

catalysis, glucose oxidase, inert polymers, poly(3,4-ethylenedioxythiophene), sensors

1 | INTRODUCTION

The incidence of diabetes, which is a major health problem for most developed societies around the world, is expected to reach 552 million people worldwide by 2030.^[1] At present time, biosensors for monitoring the glucose level in diabetic patients account for ~85% of the entire biosensor market since it is well understood that good glucose management effectively delays the progression of diabetes complications.^[2]

Glucose oxidase (GOx) is an oxidoreductase enzyme that catalyzes the oxidation of glucose to gluconolactone with consumption of oxygen and production of hydrogen peroxide.^[3] Due to its high stability and catalytic activity toward glucose, GOx is widely used for the fabrication of enzymatic base glucose biosensors.^[4] Though non-enzymatic biosensors are also being subject of numerous and successful investigations,^[5] enzymatic biosensors present a balance of advantages and disadvantages of which both are significant.

Non-enzymatic biosensors, which exploit electrochemical methods to directly oxidize glucose, present more stability, reproducibility, and also are oxygen limitation-free.^[6] Nevertheless, the electron rate of interfering species, like ascorbic acid, is usually faster than that of glucose, which seriously affects the selectivity and sensitivity of enzyme-free sensors. On the other hand, sensors based on the immobilization of GOx enzyme, which is ease of obtainment and cheap, meet accuracy requirements in major figures of merit (i.e., specificity and selectivity) since this enzyme imparts specificity and selectivity through biological recognition in environments replete of easily oxidizable species, as blood.^[7] Furthermore, materials used to immobilize GOx and transfer electrons from enzyme to electrodes are usually simpler and cheaper than those employed in non-enzymatic glucose sensing approaches that, additionally, must catalyze the oxidation of glucose. As a consequence, majority of the commercially available glucose sensors are enzyme-based.

Enzyme-based glucose sensors typically consist of an electrical conductor substrate, the GOx enzyme, and a mediator, which act as electron carrier facilitating the electron transfer between the enzyme active center and the substrate. Thus, in the case of GOx direct electron transfer is difficult to achieve since the enzyme redox center is buried inside the protein structure, and is far from any feasible substrate binding site. The mediator is usually a polymer that can be immobilized or directly polymerized onto the substrate, while the enzyme can be integrated into the polymeric matrix or directly immobilized onto the mediator surface.

In the last years, enzyme-based biosensors based on robust, accurate, and low cost electrochemical techniques are attracting a renewed interest. Thus, emerging social needs, as for example, the development of wearable and low-cost sensors,^[8] the growing number of people affected by diabetes in poor regions of the planet,^[9] and the necessity of simple and compact setups for the routine determination of glucose in blood,^[10] are creating a growing demand for simplest and cheapest sensors for the commercial implementation of home glucometers.^[11] In line with the cost-reduction, straightforward approaches, as for example, the use screen-printed^[12] and simple paper electrodes^[13] for the enzyme immobilization, have brought significant benefits.

In a very recent study, we reported on the application of corona discharge plasma technologies as a very simple and effective technology for the fabrication of sensors.^[14] More specifically, we proved that the treatment of the polymeric surfaces in a room-temperature air-discharge plasma, which is a simple and powerful means of surface modification, enables the preparation of electrochemical sensors. The most attractive advance of this technology is that sensors were achieved using not only electrochemically active conducting polymers (CPs), as for example, poly(N-methylpyrrole) and poly(3,4-ethylenedioxythiophene) (PEDOT), but also cheap

commodity plastics, which are insulating and electrochemically inert, as for example, polyethylene, polypropylene, polyvinylpyrrolidone, polycaprolactone, and polystyrene.^[14] The electrochemical response of such plasma-functionalized polymers was proved through their electrocatalytic effects of the reactive excited species on the oxidation of dopamine (DA), allowing its detections with resolution and sensitivity similar to those achieved using sensors based on sophisticated catalytic materials. DA is involved in motor and cognitive functions. The loss of DA has been associated to neurological disorders, like Parkinson's and schizophrenia.^[15]

The main aim of this work is to explore the applicability of plasma-treated low-density polyethylene (LDPE), an insulating and electrochemically inert polymer, as an effective, simple and cheap mediator for the fabrication of enzymatic glucose sensors. It is worth noting that LDPE is a very popular thermoplastic, with an annual global production of around 20 million tons, widely used in plastic packaging (e.g., shopping bags or plastic wrap). Its unique flow properties, which are especially suitable for film-based applications, low cost and recyclability, suggests that, among electrochemically inert polymers, LDPE is probably the most appropriated for the preparation of simple, low-cost, and versatile biosensing platforms. For the sake of completeness, we have also examined the performance of glucose sensors using plasma-functionalized PEDOT, a CP with excellent electrical, and electrochemical properties,^[16,17] even though such material is significantly more expensive and sophisticated than LDPE. It should be noted that the effectivity of plasma-functionalized polymers as mediators in glucose sensors (i.e., promoting the electrochemical communication between the GOx and the substrate) can be coupled with the electrocatalytic role of such treated materials in the oxidation of interferents like DA, uric acid (UA), and ascorbic acid (AA),^[14] affecting the glucose detection. Thus, such coupling has been used to propose a bifunctional biosensing platform to detect simultaneously glucose and DA. Within this context, it should be remarked that a bifunctional platform able to detect the levels of glucose and DA is highly desirable since diabetes sometimes affect the dopaminergic function, altering the motor activity regulated by dopamine activity. In order to propose such bifunctionality, we have taken advantage of the fact that UA and AA are the most important interferents of glucose and DA.

2 | EXPERIMENTAL SECTION

2.1 | Materials

3,4-Ethylenedioxythiophene (EDOT), N-(2-cyanoethyl) pyrrole (NCPy), acetonitrile, anhydrous lithium perchlorate (LiClO₄), glucose (D-glucose), DA hydrochloride (3-hydroxytyramine hydrochloride), AA (L-configuration, crystalline), UA (crystalline) of analytical reagent grade were

purchased from Sigma-Aldrich (Spain). All chemicals were used without further purification. Phosphate buffer solution (PBS) 0.1 M with $\text{pH} = 7.4$ was prepared as electrolyte solution by mixing four stock solutions of NaCl, KCl, NaHPO_4 , and KH_2PO_4 . High-purity nitrogen was used for de-aeration of the prepared aqueous solutions.

2.2 | Preparation of untreated PEDOT (U-PEDOT) electrodes

PEDOT films were prepared by chronoamperometry under a constant potential of $1.40 \text{ V}^{[17]}$ using a three-electrode two-compartment cell under nitrogen atmosphere (99.995% in purity) at 25°C . A bare glass carbon (GC) substrate with a diameter of 2 mm was used as working electrode while a steel AISI 316 sheet with an area of 1 cm^2 was employed as counter electrode. The surface of the GC was polished with alumina powder and cleaned by ultrasonication prior to the deposition of the polymer. The reference electrode was an Ag|AgCl electrode containing a 3 M KCl aqueous solution. All electrochemical experiments were conducted on a PGSTAT302N AUTOLAB potentiostat-galvanostat (Ecochimie, the Netherlands) equipped with the ECD module to measure very low current densities ($100 \mu\text{A}$ – 100 pA), which was connected to a PC computer controlled through the NOVA 1.6 software. PEDOT and films were obtained using a 10 mM monomer solution in acetonitrile with 0.1 M LiClO_4 and a polymerization time of 6 s. Accordingly, the resulting oxidized PEDOT chains are doped with perchlorate anions.

2.3 | Preparation of untreated LDPE (U-LDPE) electrodes

Plastic-modified electrodes were prepared by solvent casting. For this purpose, LDPE (34.4 mg) was dissolved in dichlorobenzene (10 mL), a volatile solvent. The resulting solution was deposited onto a bare GC substrate.

2.4 | Preparation of plasma-treated electrodes

Plasma-treated PEDOT and LDPE electrodes, hereafter denoted PT-PEDOT and PT-LDPE, respectively, were prepared with a corona discharge in ambient atmosphere using a BD-20AC from Electro-Technic Products. The treatment of the polymers was performed using a Spring Tip wire electrode and a voltage of 45 000 V at a frequency of 4.5 MHz. The time that plasma power was applied (t_{cp}) is explicitly indicated in each case.

2.5 | Scanning electron microscopy (SEM)

The surface morphology of untreated and plasma-treated samples was examined by SEM. Samples were mounted on a

double-side adhesive carbon disc and sputter-coated with a thin layer of carbon to prevent sample charging problems. Microscopy studies were carried out using a Focused Ion Beam Zeiss Neon40 scanning electron microscope equipped with an energy dispersive X-Ray (EDX) spectroscopy system and operating at 5 kV.

2.6 | FTIR and Raman spectroscopy

FTIR spectra were recorded on a FTIR Jasco 4100 spectrophotometer. Samples were placed in an attenuated total reflection accessory (Top-plate) with a diamond crystal (Specac model MKII Golden Gate Heated Single Reflection Diamond ATR). For each sample, 32 scans were performed between 4000 and 600 cm^{-1} with a resolution of 4 cm^{-1} .

Raman spectra were recorded on a HORIBAJobin Yvon LabRAM spectrometer, equipped with a 632.8 nm He-Ne laser and 0.5 mW of power.

2.7 | Contact angle

The wettability was determined using the sessile water drop method at room temperature and controlled humidity. Images of 0.5 mL distilled water drops on the electrodes were recorded after stabilization (10 s) with the equipment OCA 20 (DataPhysics Instruments GmbH, Filderstadt). The software SCA20 was used to analyze the images and acquire the contact angle value. Contact angle values were obtained as the average of 20 independent measures for each sample.

2.8 | Enzyme immobilization

Enzyme-containing glucose biosensors were prepared by immobilizing GOx untreated and plasma-treated polymers GOx. For this purpose, suitable amount of GOx solution (10 mg in 1 mL 0.1 M PBS solution) was prepared in a vial. For the immobilization onto U-LDPE, the enzyme concentration was increased to 33 mg in 1 mL 0.1 M PBS. After this, 3 μL of the GOx solution was dropped onto the untreated and plasma-treated polymer films and dried in a fridge at 6°C for 12 h. UV-vis spectroscopy measurements were carried out to probe that amount of immobilized enzyme was practically identical for all sensors.

2.9 | Electrochemical detection of glucose

Chronoamperometric measurements were carried out at room temperature, in the Autolab PGSTAT302N equipment described above, under static conditions, and using a screen-printed electrode (DRP150, from DropSens) that provides the platinum and Ag|AgCl electrode. The sample volume used during glucose and interferents addition experiments was 1–3 μL . The polarization potential was

500 mV unless other value is indicated. Chronoamperometric curves in presence of interfering agents were obtained using the same process.

Cyclic voltammetry (CV) assays were carried out to examine the oxidation peak potential of glucose. Experiments were performed using the equipment and experimental conditions described above. Voltammograms were recorded in the potential range from -0.40 to 0.80 V at a scan rate of 50 mV s $^{-1}$.

3 | RESULTS AND DISCUSSION

3.1 | Characterization of plasma-treated electrodes

In our previous work, we extensively compared the effect of plasma on bare and polymer-coated glass carbon electrodes, evidencing the indispensable role of the polymer in the electro-detection process.^[14] We characterized the chemical nature of the simple excited species formed upon exposure of PEDOT and LDPE electrodes to corona discharge-plasma (CD-plasma) using X-ray photoelectron spectroscopy (XPS).^[14] More specifically, we proved the formation of a large variety of reactive species at the surface (e.g., N, O, N $_2^+$, O $_2^+$, and O $^+$), which catalyzed the DA oxidation promoting its detection. Furthermore, XPS measurements reflected that plasma exposure induces functionalization of the polymeric surface. Thus, the mechanism proposed for this functionalization process can be summarized as follows:^[14] (i) the interaction of the polymer surface with the plasma induces hydrogen separation from polymeric chains and free radical creation; (ii) radicals created by such plasma activation interact with oxygen and nitrogen from air and/or with the reactive species previously mentioned, which are adsorbed in the polymeric matrix; and (iii) new functional groups arisen from such interactions are incorporated into the polymer surface, which becomes very active. XPS results clearly indicated that the nature of reactive species formed upon exposure of the polymer to the plasma depends on both the chemical structure and the duration of the treatment. In this section, we expand the characterization of PT-PEDOT and PT-LDPE using SEM, FTIR, and Raman spectroscopies, and contact angle measurements. Thus, our main goal was to identify differences between such two plasma-treated systems, which obviously depend on the chemical structure of the source polymer.

Figure 1 displays U-PEDOT and U-LDPE electrodes as well magnified SEM micrographs of the surface morphology before and after plasma treatment. The GC substrate is completely coated in both cases (Figure 1a). However, the surface morphology of two polymers is radically different before

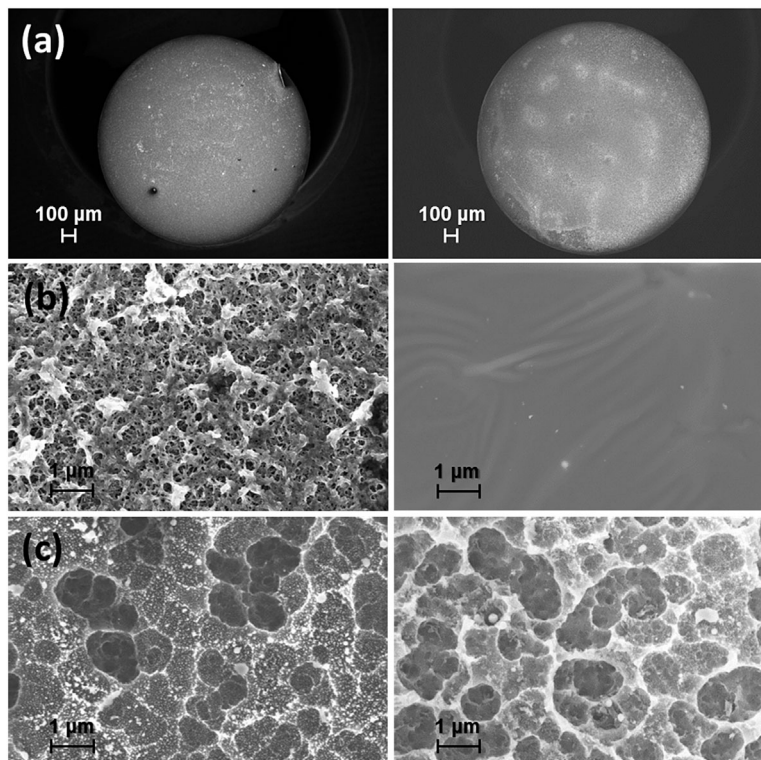


FIGURE 1 SEM micrographs of PEDOT (left) and LDPE (right) electrodes: (a) Completely image of the GC substrate coated with polymer; (b) high resolution image of the polymers before plasma treatment; and (c) high resolution image of the polymers after plasma treatment. In all cases, plasma treatment was conducted using $t_{cp} = 1$ min

plasma treatment (Figure 1b). Thus, U-PEDOT consists on homogenous distribution of clusters and sticks connected forming a relatively porous network with narrow and tortuous pores, which are typically used to explain the excellent electrochemical properties observed for PEDOT.^[18] In contrast, U-LDPE presents a very smooth and compact morphology, in which no pore is detected at the surface. After the plasma treatment ($t_{cp} = 1$ min), the surface of the two electrodes, which can be described as an abundant and homogeneous distribution of ~ 1 μ m aggregates, becomes very similar identical (Figure 1c). Moreover, aggregates are separated by pores, which lost the tortuosity of those observed for U-PEDOT. This morphological change is expected to facilitate not only the diffusion of ions but also the electron transfer during electrochemical processes, especially in the case of plasma-treated LDPE. It should be mentioned that, although the film thickness was not severely affected by the plasma (i.e., it decreased around 20% only), the film fragility increased considerably for both PEDOT and LDPE.

Figure 2a compares the FTIR spectra of the EDOT monomer, U-PEDOT, and PT-PEDOT ($t_{cp} = 1$ min). The monomer spectrum displays intense and sharp characteristic bands at 1482 cm $^{-1}$ (asymmetric C=C aromatic stretching), 1363 cm $^{-1}$ (C-C and C=C stretches of the thiophene ring),

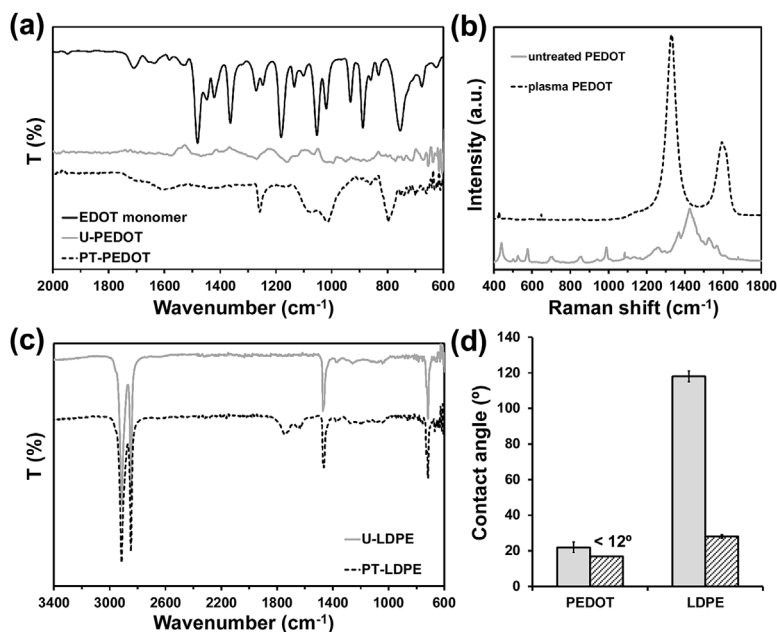


FIGURE 2 (a) FTIR spectra of EDOT, U-PEDOT, and PT-PEDOT. (b) Raman spectra of U-PEDOT and PT-PEDOT. (c) FTIR spectra of U-LDPE and PT-LDPE. (d) Water contact angle for untreated (solid gray) and plasma-treated (dashed) PEDOT and LDPE. In all cases, plasma treatment was conducted using $t_{cp} = 1$ min

1181 cm⁻¹ (C—O—C bending), 1053 cm⁻¹ (C—O stretching), 932 cm⁻¹ (C—S stretching), and 753 cm⁻¹ (C^α—H out of plane bending). For U-PEDOT films the bands are considerably weaker than for the monomer due to the strong interactions with the dopant agent. In spite of this, the bands associated with the C—O—C bending, C—O stretching, and C—S stretching are identified at 1159, 1061, and 950 cm⁻¹, respectively. Although the spectrum of PT-PEDOT evidences the formation of reactive species at the surface, the assignment of the bands is not an easy task due to their broadness. In spite of this, the presence of secondary cyclic alcohols is reflected by the intense peaks at 1080 and 1013 cm⁻¹, while the C—O ether stretching shows a shift decreasing from 1266 cm⁻¹ (in the monomer and U-PEDOT) to 1259 cm⁻¹. To further investigate the mechanism of chemical change in PEDOT films after plasma treatment, Raman spectra were collected (Figure 2b). Before the plasma treatment, PEDOT exhibits a strong absorption band at 1436 cm⁻¹, which corresponds to the symmetric C=C stretching. Besides, several kinds of characteristic bands are detected at 1523, 1370, 1257, and 987 cm⁻¹ are related to the anti-symmetrical C^α—C^α and C^β—C^β stretching, deformation in the C—O—C bond and ring deformation, respectively.^[19] After plasma treatment, these bands shows significant changes in shape, position, and intensity. More specifically, two very strong bands centered at 1342 and 1592 cm⁻¹ apparently group the C—C and C=C bands, reflecting a very drastic change in the resonant structure of the polymer chains.^[20]

Figure 2c displays the FTIR spectrum of U-LDPE, which exhibits two large and sharp absorption bands at 2912 and 2847 cm⁻¹ due to asymmetric and symmetric C—H stretching vibrations, respectively.^[21] Furthermore, the less intense peaks at 1470 and 717 cm⁻¹, which are associated to the C—H deformation and C—C rocking vibrations in $-(CH_2)_n-$, respectively, are also clearly identified. Figure 2c, which includes the FTIR spectrum of PT-LDPE, shows that the above mentioned peaks are maintained after plasma treatment. However, a broad band arising from the C=O stretching of ketones, aldehydes, and/or carboxylic acids, appears at 1737 cm⁻¹. Moreover, a band at 1644 cm⁻¹, which could be attributed to the presence of C=C bonds (C=C stretching vibration), is also identified. Thus, comparison of the two spectra shown in Figure 2c clearly reflects that plasma treatment promotes the formation of oxygen-containing functionalities and vinyl groups on the polymer surface of LDPE, which is in agreement with previous observations.^[14,22]

Comparison of the spectra recorded for PT-PEDOT and PT-LDPE reflect some differences not only in the formed oxygen-containing functionalities but also in the carbonaceous species. It is worth noting that these variations did not affect the detection of DA since the excited species responsible of the electrocatalytic oxidation of such neurotransmitter were proved to be present in both plasma-treated polymers (i.e., the detection of DA using plasma-treated polymers was found to be practically independent of the source polymer).^[14] However, chemical differences can play a crucial role in the effectivity electron transfer processes, which is essential for the communication between the enzyme and the GC substrate. Therefore, the chemical nature of the source polymer could affect to its effectivity as mediator in glucose detection. The water contact angle (θ) values determined for untreated and plasma-treated polymers are displayed in Figure 2d. PEDOT is a hydrophilic CP while LDPE exhibits lipophilic character. Application of the CD-plasma ($t_{cp} = 1$ min) results in an enhancement of the wettability, which is particularly noticeable for LDPE. Thus, θ decreases from $118 \pm 3^\circ$ to $28 \pm 3^\circ$, transforming this polyolefin into very hydrophilic material. These results support that, despite the chemical differences in terms of functionalization observed by spectroscopy, the two plasma-treated polymer surfaces contain charged species.

3.2 | Glucose detection

GOx was immobilized onto both untreated and plasma-treated electrodes for comparison. This process was very successful for electrodes with hydrophilic surfaces (i.e.

U-PEDOT, PT-PEDOT, and PT-LDPE in Figure 2d), an enhancement of the enzyme concentration being required for the enzyme immobilization onto lipophilic U-LDPE (see Experimental section). Although the enzyme concentration deposited on U-LDPE was three times higher than that on the other substrates, the concentration of GOx concentration immobilized onto the surface was similar in all cases. Accordingly, this variation in the concentration of the dropped solution is not expected to affect the interpretation of the electrochemical detection results. Hereafter, untreated and plasma-treated enzyme-containing polymeric electrodes have been denoted U-PEDOT/GOx, U-LDPE/GOx, PT-PEDOT/GOx, and PT-LDPE/GOx, depending on the polymer used for their preparation.

The electrochemical response of 10 mM glucose in 0.1 M PBS (pH = 7.4) was examined by CV at both untreated and plasma-treated electrodes. Voltammograms recorded using U-PEDOT, PT-PEDOT, U-PEDOT/GOx, and PT-PEDOT/GOx electrodes are compared in Figure S1a. The glucose in contact with the U-PEDOT/GOx shows a well resolved peak potential at 0.36 V, while PT-PEDOT/GOx detects the electrochemical oxidation of glucose by a weak shoulder at 0.50 V. Non-enzymatic electrodes do not allow the detection of glucose since oxidation peaks (U-PEDOT) or shoulders (PT-PEDOT) are not appreciated. On the other hand, voltammograms registered at PT-LDPE/GOx electrodes prepared by applying different times of plasma power ($t_{cp} = 30$ s, 1 and 2 min) allow detection of glucose oxidation by a shoulder at 0.50 V (Figure S1b), while no electrochemical process was observed at U-LDPE/GOx. The latter observation is consistent with the insulating properties of LDPE, which preclude the electrochemical communication between the enzyme and the GC substrate. Overall, CV results displayed in Figure S1 were used to fix the polarization potential at 0.50 V for the chronoamperometric measurements with plasma-treated electrodes.

Figure 3a shows the typical current-time plots of the U-PEDOT/GOx and PT-PEDOT/GOx ($t_{cp} = 1$ and 2 min) sensors on successive addition of 1 mM glucose into a continuously stirred solution. The response of the plasma-treated sensors was faster than that of U-PEDOT/GOx, the formers achieving 95% of the maximum steady-state response in less of 8 s. The response current increased with the concentration of glucose in the medium, Figure 3b showing the calibration plot of the current time response of the three sensors and the corresponding calibration equation. Table 1 lists the linear dynamic range (LDR), the limit of the detection (LOD) and the sensitivity of the three enzymatic PEDOT-based sensors

The LDR clearly depends on the plasma treatment (Table 1). Thus, the LDR displayed by U-PEDOT/GOx is very short, spanning up to 4 mM (Figure 3b). At higher concentrations, the signal saturates. This behavior is fully

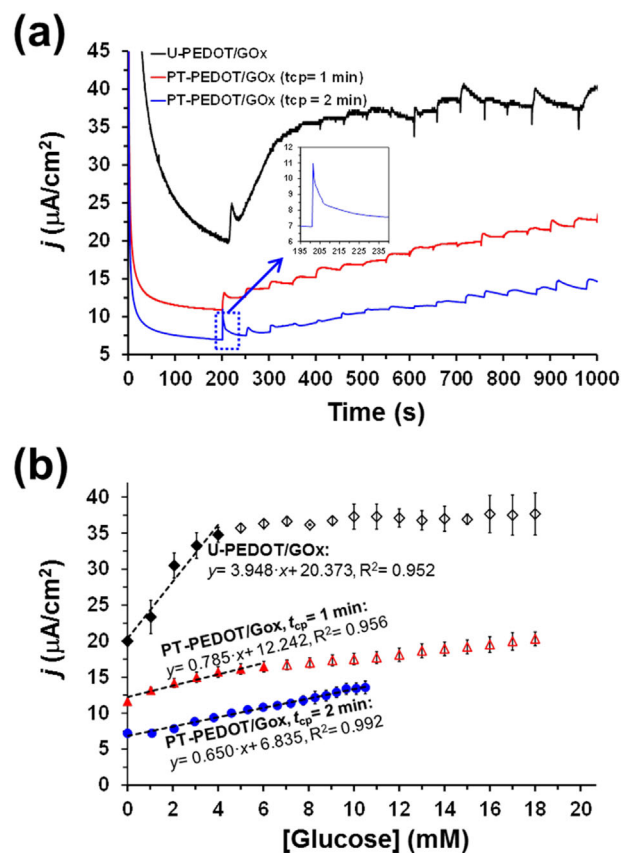


FIGURE 3 (a) Current-time plots for the U-PEDOT/GOx and PT-PEDOT/GOx ($t_{cp} = 1$ and 2 min) upon the successive addition in 0.1 M PBS of 1 mM glucose. Polarization potential: 0.50 V versus Ag|AgCl. (b) Current density response versus glucose concentration for the three sensors mentioned above. Error bars indicate standard deviations for five measurements using independent electrodes. The calibration curve equation is also displayed

consistent with that observed for other enzymatic PEDOT electrodes for glucose detection, in which GOx was entrapped into the polymeric matrix by considering a polymerization medium with both the enzyme and the EDOT monomer.^[23] The interval of glucose concentration over which the sensor response is linear is higher for PT-PEDOT/GOx than for U-PEDOT/GOx. Moreover, the LDR interval grows when the t_{cp} increases from 1 to 2 min (Table 1). Besides, the LOD and the sensitivity increases and decreases, respectively, when the PEDOT electrodes are exposed to plasma. Accordingly, PT-PEDOT/GOx systems are slightly less precise and sensitive than U-PEDOT/GOx. This observation points out that, although the electrical communication between the catalytic enzyme and the GC substrate is faster for plasma-treated electrodes, it becomes definite and efficient when aromatic polymer chains at the surface transform into reactive species. In spite of this, it is worth noting that the sensitivity and precision of PT-PEDOT/GOx electrodes is comparable to other sensors reported in the literature. For example, the LOD

TABLE 1 Linear dynamic range (LDR), limit of detection (LOD) and sensitivity (S) of the untreated and plasma treated sensors studied in this work. The time that plasma power was applied (t_{cp}) is indicated for plasma-treated sensors

Sensors	LDR (mM)	LOD (mM)	S ($\mu\text{A} \cdot \text{cm}^{-2} \cdot \text{mM}^{-1}$)
U-PEDOT/GOx	0–4	0.44	3.95
PT-PEDO/GOx (t_{cp} = 1 min)	0–6	0.81	0.78
PT-PEDO/GOx (t_{cp} = 2 min)	0–10.5	1.40	0.65
U-LDPE/GOx	–	–	–
PT-LDPE/GOx (t_{cp} = 30 s)	0–20	0.9	0.54
PT-LDPE/GOx (t_{cp} = 1 min)	0–20	1.3	0.96
PT-LDPE/GOx (t_{cp} = 2 min)	0–20	1.7	1.31

of non-enzymatic sensors based on polythiophene derivatives ranged from 0.2 to 6.2 mM while the LDR was very similar to those displayed in Table 1 (i.e., from 0 to 6–9 mM).^[5b,24]

On the other hand, additional amperometric assays on successive addition of 1 mM glucose were performed for PT-PEDOT/GOx sensors using a polarization potential of 0.36 V, which corresponds to the glucose oxidation peak potential identified by CV for U-PEDOT/GOx (Figure S1a) sensors. Results proved that glucose is not clearly detected at such potential (Figure S2). Thus, the response current does not increase with the concentration of glucose in the medium, which is in agreement with the voltammograms recorded for PT-PEDOT/GOx (Figure S1a).

Results obtained for U-LDPE/GOx and PT-LDPE/GOx electrodes, which were prepared considering t_{cp} = 30 s, 1 and 2 min, are displayed in Figure 4a. As it was expected, the U-LDPE/GOx electrode is not able to detect the oxidation of glucose, independently of the concentration. Thus, LDPE is an electrical insulator, hindering the transfer of electrons from GOx to the GC substrate. In contrast, application of plasma treatment results in a linear regime that is consequence of the role played by the reactive species formed on the surface as electron transfer mediator. Moreover, the electrical communication between GOx and the GC substrate increases with the t_{cp} . This behavior is the opposite of that observed for PEDOT-based electrodes, in which the electron transfer was more efficient for U-PEDOT/GOx than for PT-PEDOT/GOx, the efficiency of the latter decreasing with increasing t_{cp} . However, the response is slower for PT-PEDOT/GOx (i.e., around 45 s) than for U-PEDOT/GOx.

Inspection of Table 1 reveals that the LOD and the sensitivity increase from 0.9 to 1.7 mM and from 0.54 to

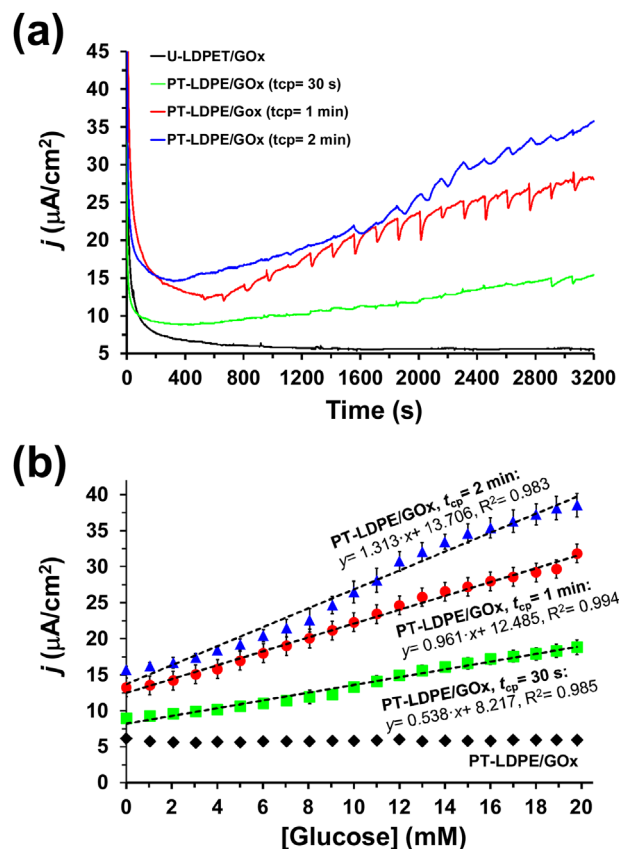


FIGURE 4 (a) Current-time plots for the U-LDPE/GOx and PT-LDPE/GOx (t_{cp} = 30 s, 1 and 2 min) upon the successive addition in 0.1 M PBS of 1 mM glucose. Polarization potential: 0.50 V versus Ag|AgCl. (b) Current density response versus glucose concentration for the three sensors mentioned above. Error bars indicate standard deviations for five measurements using independent electrodes. The calibration curve equation is also displayed

1.31 $\mu\text{A} \cdot \text{cm}^{-2} \cdot \text{mM}^{-1}$, respectively, when t_{cp} grows from 30 s to 2 min. These results suggest that reactive species formed on the LDPE probably undergo decomposition when t_{cp} exceeds a threshold value. However, all these values are within the accepted interval for glucose detection. On the other hand, in spite of PT-LDPE/GOx obtained using t_{cp} = 30 s provides the best detection performance, the linearity of the profile obtained using t_{cp} = 1 min is the highest with $R^2 > 0.99$ (Figure 4b). However, all PT-LDPE/GOx sensors show good linearity, independently of t_{cp} , the LDR spanning up to 20 mM.

Results presented in this sub-section reflect significant differences in the behavior of the two examined plasma-treated polymers, which are in opposition with respect to previous observations as dopamine detectors.^[14] In the latter case, the high reactivity of the excited species formed on the surface of the two polymers had direct electrocatalytic effects in the oxidation of dopamine to dopamine-*o*-quinone. Considering that the sensitivities for the determination of

dopamine were comparable for both polymers, we concluded that the reactive species responsible of such electrocatalytic reactions were the same for plasma-treated PEDOT and LDPE. In contrast, the role of the polymers in enzymatic glucose sensors is the establishment of efficient electrical communication between the GOx and the GC surface. Accordingly, U-PEDOT, which is a semi-conductor, facilitates the diffusion of electrons, while insulating U-LDPE hinders it. The reactive species formed on the surface of PT-PEDOT affect the π -electron delocalization, decreasing the electronic conduction. In opposition, some of the excited species formed on the surface of PT-LDPE can diffuse through the polymeric matrix, which results in an enhancement of the electrical conductivity due to the ions mobility. These features are fully consistent with spectroscopic differences displayed in Figure 2 for PT-PEDOT and PT-LDPE, explaining the parameters listed in Table 1 and, especially, the good results obtained when PT-LDPE films are used as electrochemical mediators for electron transfer in enzymatic glucose sensors.

3.3 | Selectivity toward the electrocatalytic oxidation of interferents

This selectivity of the PT-LDPE/GOx sensor prepared using $t_{cp} = 1$ min is evidenced in Figure 5, which displays the control voltammogram of 10 mM glucose in 0.1 M PBS with 0.1 mM DA, 0.1 mM AA, and 0.1 mM UA at PT-PEDOT/GOx ($t_{cp} = 1$ min). It is worth noting that three species, which glucose, DA and UA with peak potentials at 0.34, 0.17, and 0.55 V, respectively, exhibit very well resolved oxidations. However, the oxidation of AA only causes a small shoulder at a potential of 0.02 V, indicating that the sensitivity toward this interferent is clearly lower than toward DA and UA. The peak anodic current for glucose, DA, AA, and UA are 2.84, 3.80, 0.73, and 3.02 μA /

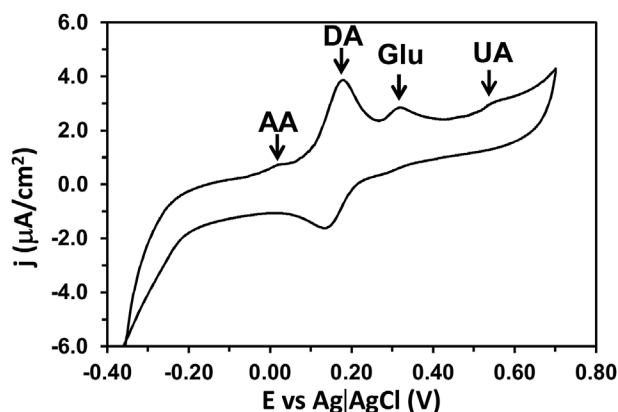


FIGURE 5 Cyclic voltammogram at PT-LDPE/GOx sensor ($t_{cp} = 1$ min) of 10 mM glucose in 0.1 M PBS with 0.1 mM DA, 0.1 mM AA, and 0.1 mM UA. Scan rate: 50 mV s^{-1}

cm^2 , respectively. In spite of the low sensitivity toward AA, it should be emphasized that the oxidation of this interferent occurs at a potential that is clearly different from those observed for the oxidations of glucose, DA and AA. Therefore, although the sensitivity of the PT-LDPE/GOx sensor toward AA is very low with respect to the other analytes, it should be remarked that it works selectively because of separation between the oxidation peaks is clear and well-resolved.

The presence of interfering species, such as UA, AA, and DA in biological samples can influence the performance of the enzymatic sensor during the oxidation of glucose. In order to investigate the selectivity of plasma treated polymers, the chronoamperometric response of the PT-PEDOT/GOx and PT-LDPE/GOx enzymatic sensors upon the successive injection of interferents and glucose into the PBS-containing cell was examined. Two different sets of experiments were carried out. In the first one, *set#1*, the concentrations of all added species (i.e., interferents and glucose) was 1 mM, while in the second one, *set#2*, the concentrations of the added interferents were reduced to 0.1 mM while that of glucose was kept at 1 mM. It is worth noting that the concentration or variety of species contained in the analyzed solution change upon each injection by accumulation. Ideally, sensors should be able to detect the analyte and the interferents (selectivity), exhibiting an increment of intensity with the concentration of analyte (sensitivity) but not necessarily with the concentration of interferents. Unfortunately, sensors are not ideal and the final choice is a compromise between selectivity and sensitivity.

Results obtained for PT-PEDOT/GOx ($t_{cp} = 1$ and 2 min) are displayed in Figure 6. It should be mentioned that the displayed profiles are representative because of their reproducibility using different and independently prepared PT-PEDOT/GOx sensors. As it can be seen, the oxidation of all the injected species, glucose and interferents, is clearly detected by such sensors. Furthermore, the current density tends to increase with the injection of the glucose, even though this behavior is clearer when the concentration of interferents is low. When the concentration of the added species is 1 mM (*set#1*), the chronoamperometric response toward glucose is quite selective with respect to the addition UA and AA, and less selective with respect to the injection of DA (Figure 6a), especially when $t_{cp} = 2$ min. However, the latter drawback is much less important when the concentrations of interferents decrease to 0.1 mM (Figure 6b), even though the intensity of their signals is very high with respect to that measured for injected glucose. The latter feature indicates that the electron rate of DA, UA, and AA is faster than that of glucose.

In general, the behavior displayed in Figure 6 should be attributed to the co-existence of two catalytic processes: (i) the oxidation of glucose to gluconolactone, which is catalyzed by the GOx; and (ii) the oxidation of DA, UA, and AA, which is electrocatalyzed by the plasma activated PEDOT surfaces.^[14] Accordingly, PT-PEDOT/GOx should be considered

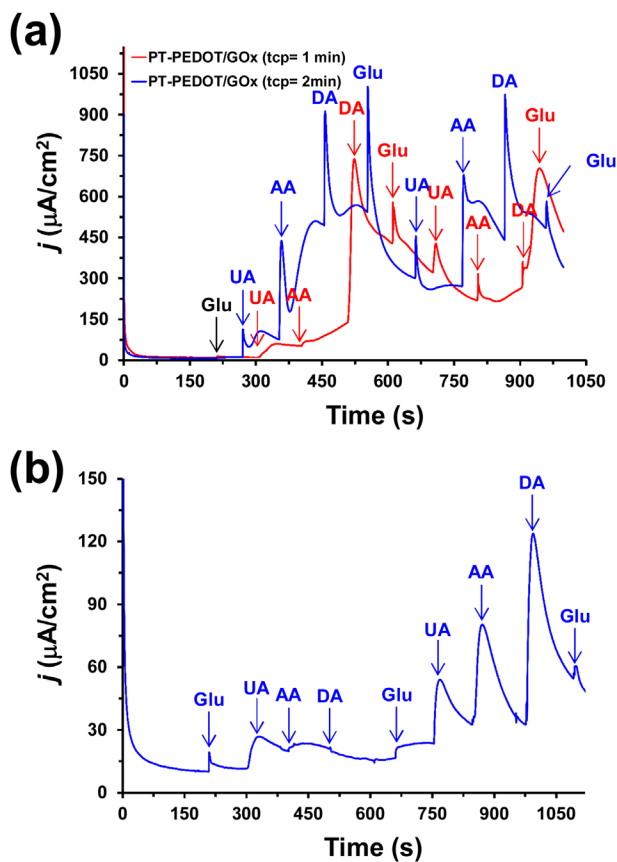


FIGURE 6 Current-time plots for the PT-PEDOT/GOx sensors ($t_{cp} = 1$ min and 2 min in red and blue, respectively) upon the successive addition in 0.1 M PBS of: (a) 1 mM glucose, 1 mM UA, 1 mM AA, and 1 mM DA (*set#1*); (b) 1 mM glucose, 0.1 mM UA, 0.1 mM AA, and 0.1 mM DA (*set#2*). Polarization potential: 0.50 V versus Ag|AgCl

bifunctional catalysts electrodes for the selective detection of glucose and DA (i.e., in presence of UA and AA). Nevertheless, as discussed in previous sub-section, the performance of PT-PEDOT films as mediators in enzymatic sensors exhibits some drawbacks (Figure 3), which clearly affects this bifunctionality, in particular the selectivity. These limitations are overcome by PT-LDPE/GOx sensors, as it is reflected in Figure 7.

The chronoamperometric response to the glucose and interferents injection of PT-LDPE/GOx sensors was significantly clearer than that of PT-PEDOT/GOx for both *set#1* and *set#2*. This is particularly noticeable for systems with mediators based PT-LDPE films produced using $t_{cp} = 1$ min (Figure 1). In this case, the peaks associated to the injection of glucose, DA, UA, and AA are not only well and clearly resolved, but also exhibit very different current densities, evidencing that PT-LDPE/GOx with $t_{cp} = 1$ min act as efficient bifunctional sensors for the selective detection of glucose and DA. As occurred above for PT-PEDOT/GOx the lowest current density corresponds to the injection of glucose. This feature confirms that the electron transfer rate is slower when the oxidation occurs at the active center of the enzyme, which

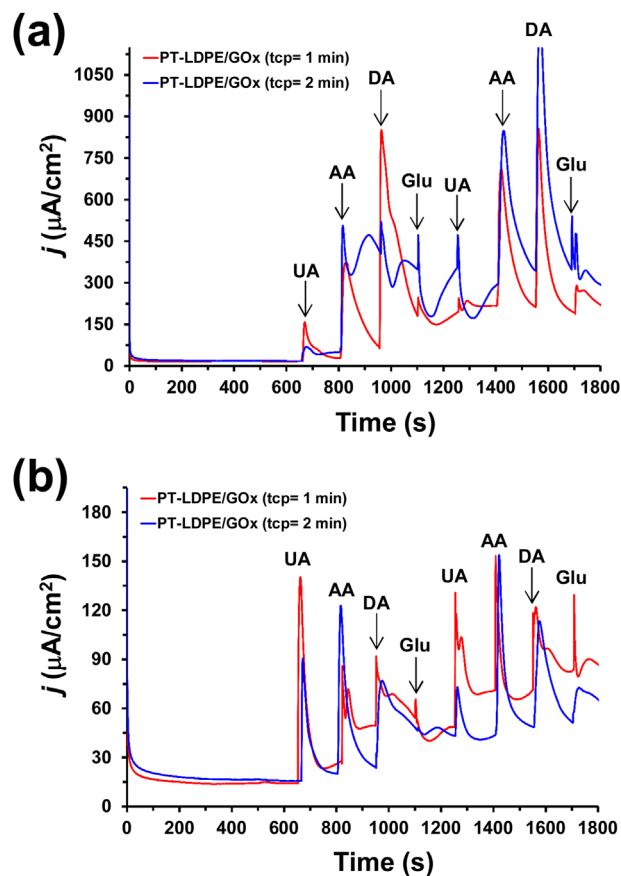


FIGURE 7 Current-time plots for the PT-LDPE/GOx sensors ($t_{cp} = 1$ and 2 min in red and blue, respectively) upon the successive addition in 0.1 M PBS of: (a) 1 mM glucose, 1 mM UA, 1 mM AA, and 1 mM DA (*set#1*); (b) 1 mM glucose, 0.1 mM UA, 0.1 mM AA, and 0.1 mM DA (*set#2*). Polarization potential: 0.50 V versus Ag|AgCl

in turn is immobilized onto the surface of the mediator, than when it directly takes place onto the surface of the mediator.

Results indicate that the intrinsic electrocatalytic activity of PT-LDPE is preserved when GOx enzymes are immobilized onto the surface. Moreover, the role as mediator of PT-LDPE in glucose sensors does not interfere with the electrocatalytic oxidation of DA, differences between electron transfer rates of the species oxidized in the active center of the enzyme and onto the surface of PT-LDPE allowing discrimination. Overall, the proposed bifunctional sensor has significant advantages, especially those related with the low cost of the polymer and the simplicity of the processes required for its transformation and treatment (i.e., solvent casting and CD-plasma application, respectively).

4 | CONCLUSION


Results obtained in this work demonstrate that PT-LDPE can be utilized as very simple, low-cost and versatile platform for biosensors fabrication. More specifically, bifunctional sensors have been constructed by applying CD-plasma power during

1 min onto the surface of LDPE films, which were previously deposited by solvent-casting onto the surface of GC substrates. After this, the GOx is immobilized onto the PT-LDPE surface by physical adsorption. Plasma treatment transforms LDPE, which is an electrochemically inert and electrically insulating polymer, into an electrochemically active material able to participate in electron transfer processes, coupling the electrocatalytic activity required for the oxidation of DA to the role as the mediator necessary for the communication between the enzyme responsible of the glucose oxidation and the GC substrate. Both glucose and DA, which exhibit very different electron transfer rates, can be clearly differentiated from the rest of interferents. Future work is oriented toward the optimization of this bifunctional sensor, which should detect selectively the two biomolecules in a single measurement.

ACKNOWLEDGMENTS

Authors acknowledge MINECO/FEDER (MAT2015-69367-R) for financial support. G.F. is thanked for the financial support through a postdoc-UPC. J.L. is Serra Hünter Fellow. J.L. and C.A. are grateful to ICREA Academia program.

ORCID

Carlos Alemán  <http://orcid.org/0000-0003-4462-6075>

REFERENCES

- [1] D. W. N. Unwin, L. Guariguata, G. Ghyoot, D. Ga, *Diabetes Atlas*, 5th ed., International Diabetes Federation, Brussels, Belgium **2012**.
- [2] S. K. Mahadeva, J. Kim, *Sens. Actuators B Chem.* **2011**, *157*, 177.
- [3] 3a P. Kavanagh, D. Leech, *Phys. Chem. Chem. Phys.* **2013**, *15*, 4859; 3b E. Tremey, E. Suraniti, O. Courjean, S. Gounel, C. Stines-Chaumeil, F. Louerat, N. Mano, *Chem. Commun.* **2014**, *50*, 5912.
- [4] 4a V. Vamvaki, K. Tsagaraki, N. Chaniotakis, *Anal. Chem.* **2006**, *78*, 5538; 4b X. A. Xu, S. J. Jiang, Z. Hu, S. Q. Liu, *ACS Nano* **2010**, *4*, 4292; 4c J. C. Yu, Y. J. Zhang, S. Q. Liu, *Biosens. Bioelectron.* **2014**, *55*, 307; 4d K. Ramachandran, T. R. Kumar, K. J. Babu, G. G. Kumar, *Sci. Rep.* **2016**, *7*, 36583.
- [5] 5a S. A. Zaidi, J. H. Shin, *Talanta* **2016**, *149*, 30; 5b M. Hocevar, G. Fabregat, E. Armelin, C. A. Ferreira, C. Alemán, *Eur. Polym. J.* **2016**, *79*, 132; 5c H. Zhu, L. Li, W. Zhou, Z. P. Shao, X. J. Chen, *J. Mater. Chem. B* **2016**, *4*, 7333; 5d P. Kannan, T. Maiyalagan, E. Marsili, S. Ghosh, J. Niedzioka-Jonsson, M. Jonsoon-Niedziolka, *Nanoscale* **2015**, *8*, 843; 5e P. Kannan, C. S. Rout, *Chem. Eur. J.* **2015**, *21*, 9355.
- [6] S. Park, H. Boo, T. D. Chung, *Anal. Chim. Acta* **2006**, *556*, 46.
- [7] 7a J. D. Newman, S. J. Setford, *Mol. Biotechnol.* **2006**, *32*, 249; 7b S. B. Bankar, M. V. Bule, R. S. Singhal, L. Ananthanarayan, *Biotech. Adv.* **2009**, *27*, 489.
- [8] 8a A. J. Bandonkar, I. Jeeran, J. Wang, *ACS Sens.* **2016**, *1*, 464; 8b E. J. Maxwell, A. D. Mazzeo, G. M. Whitesides, *MRS Bull.* **2013**, *38*, 309.

- [9] J. E. Shaw, R. Sicree, P. Z. Zimmet, *Diabetes Res. Clin. Pract.* **2010**, *87*, 4.
- [10] L. Li, Y. Wang, L. Pan, Y. Shi, W. Cheng, Y. Shi, G. Yu, *Nano Lett.* **2015**, *15*, 1146.
- [11] M. Invernale, M. B. C. Tang, R. L. York, L. Le, D. Y. Hou, D. G. Anderson, *Adv. Healthcare Mater.* **2014**, *3*, 1.
- [12] 12a O. D. Renedo, M. Alonso-Lomillo, M. J. A. Martínez, *Talanta* **2007**, *73*, 202; 12b S. S. Kamanin, V. A. Arlyapov, T. V. Rogova, A. N. Reshetilov, *Appl. Biochem. Microbiol.* **2014**, *60*, 835.
- [13] 13a Z. Nie, C. Nijhuis, J. Gong, X. Chen, A. Kumachev, A. W. Martinez, M. Narovlyansky, G. M. Whitesides, *Lab Chip* **2010**, *10*, 477; 13b M. Marilla, R. Canovas, F. J. Andrade, *Biosens. Bioelectron.* **2017**, *90*, 110.
- [14] G. Fabregat, J. Osorio, A. Castedo, E. Armelin, J. J. Buendía, J. Llorca, C. Alemán, *Appl. Surf. Sci.* **2017**, *399*, 638.
- [15] 15a E. R. Kandel, J. H. Schwartz, T. M. Jessel, *Principles of Neural Science*, 4th ed., McGraw-Hill, New York **2000**. pp. 207–298; 15b B. J. Venton, R. M. Wightman, *Anal. Chem.* **2003**, *75*, 414A.
- [16] 16a L. B. Groenendaal, F. Jonas, D. Freitag, H. Pielartzik, J. R. Reynolds, *Adv. Mater.* **2000**, *12*, 481; 16b S. Kirchmeyer, K. Reuter, *J. Mater. Chem.* **2005**, *15*, 2077; 16c L. Pettersson, T. Johansson, F. Carlsson, H. Arwin, O. Inganas, *Synth. Met.* **1999**, *101*, 198.
- [17] C. Ocampo, R. Oliver, E. Armelin, C. Alemán, F. Estrany, *J. Polym. Res.* **2006**, *13*, 193.
- [18] D. Aradilla, F. Estrany, C. Alemán, *J. Phys. Chem. C* **2011**, *115*, 8430.
- [19] S. Garreau, G. Louarn, J. P. Buisson, G. Froyer, S. Lefrant, *Macromolecules* **1999**, *32*, 6807.
- [20] T.-W. Kim, H.-Y. Woo, W.-G. Jung, D.-W., J.-Y. Kim, *Thin Solid Films* **2009**, *517*, 4147.
- [21] G. Socrates, *Infrared and Raman Characteristic Group frequencies Tables and Charts*, 3rd ed., John Wiley & Sons, West Sussex **2001**.
- [22] 22a L. J. Gerenser, *J. Adhes. Sci. Technol.* **1987**, *1*, 303; 22b F. Clouet, M. K. Shi, *J. Appl. Polym. Sci.* **1992**, *46*, 1955.
- [23] P.-C. Nien, T.-S. Tung, K.-C. Ho, *Electroanalysis* **2006**, *18*, 1408.
- [24] 24a H. Çiftçi, U. Tarmer, *React. Funct. Polym.* **2012**, *72*, 127; 24b F. Meng, W. Shi, Y. Sun, X. Zhu, G. Wu, C. Ruan, X. Liu, D. Ge, *Biosens. Bioelectron.* **2013**, *42*, 141; 24c H. Çiftçi, U. Tarmer, *Electrochim. Acta* **2013**, *90*, 358.

SUPPORTING INFORMATION

Additional Supporting Information may be found online in the supporting information tab for this article.

How to cite this article: Buendía JJ, Fabregat G, Castedo A, Llorca J, Alemán C. Plasma-treated polyethylene as electrochemical mediator for enzymatic glucose sensors: Toward bifunctional glucose and dopamine sensors. *Plasma Process Polym.* 2018;15:e1700133.
<https://doi.org/10.1002/ppap.201700133>